

## Si diffusion behavior during laser welding-brazing of Al alloy and Ti alloy with Al-12Si filler wire

CHEN Shu-hai(陈树海), LI Li-qun(李俐群), CHEN Yan-bin(陈彦宾), LIU De-jian(刘德健)

State Key Laboratory of Advanced Welding Production Technology,  
Harbin Institute of Technology, Harbin 150001, China

Received 11 June 2008; accepted 9 July 2009

**Abstract:** In laser welding-brazing of Al alloy (5A06) and Ti alloy (Ti-6Al-4V) with rectangular CO<sub>2</sub> laser spot and with Al-12Si filler wire, element Si enriches at the interface between Ti substrate and the filler metal. It is found that the Si diffusion behavior has a significant effect on the formation of interfacial intermetallic compounds. To analyze the Si diffusion behavior, a model for the prediction of the chemical potential for ternary alloy was established. According to the calculated results of the influence of the element content and temperature in Ti-Al-Si system on Si chemical potential, the diffusion behavior of Si element was analyzed for Ti dissolution and melting mode, which presents a good agreement with the experimental data. Further, formation mechanism of the interfacial intermetallic compound was clarified.

**Key words:** laser welding-brazing; diffusion behavior; chemical potential; interfacial reaction

### 1 Introduction

In aircraft industry, hybrid structures of titanium and aluminum alloys could offer advantages in comparison with conventional materials[1–2]. The performances of Ti and Al have great differences in crystal microstructure, melting point, heat conductivity, coefficient of linear expansion, etc., so the joining of Al alloy to Ti alloy is difficult when applying the traditional fusion method. The dissimilar combination of titanium and aluminum has been realized by diffusion welding[3–4], vacuum brazing[5–6], friction welding[7] and explosion welding[8]. However, above welding methods are restricted by joint configuration or vacuum condition. In additional, low mechanical strength for the joints is another problem for these methods.

A key issue encountered in joining aluminum to titanium is the formation of interfacial intermetallic phases, which depends on the process related temperature–time cycles. Due to its high energy density and cooling velocity, laser is suitable as the heat source of the controlling interfacial reaction in joining Al to Ti. To achieve laser joining of Al alloy to Ti alloy, while fusion joint is formed by melting aluminum and filler

wire Al-12Si, brazing joint is formed by molten filler and solid titanium. Therefore, a reliable joining could be achieved with this method called “laser welding-brazing” by controlling effectively the interfacial reaction. Previous works indicated that good results of the welding are obtained and tensile strength of the joints can exceed that of most Al alloys[9–10].

Compared with brazing and diffusion-bonding, complex metallurgical reaction and diffusion process of elements appear due to fast heating and cooling velocities of the laser welding at the interface. It is found that both modes of Ti melting and dissolution, which depend on the heat input, exhibited in welding-brazing. In addition, the diffusion behavior of Si element has significant influence on interfacial reaction mechanism. Therefore, according to established prediction model of the chemical potential for the Ti-Al-Si system, the effect of the element content and temperature on Si chemical potential was analyzed. Further, Si diffusion behavior and interfacial reaction mechanism in both modes of Ti melting and dissolution were clarified.

### 2 Experimental

Non-uniform heating and small heating area are

disadvantageous to melt stably filler wire and wet base metal. Therefore, laser beam was modulated to rectangular spot (focal spot size of  $2\text{ mm} \times 4\text{ mm}$ ) by the integral mirror to get more uniform energy distribution. To improve further the spreadability, V-shape groove with  $45^\circ$  angle was fabricated on base metal. Double shielding gas argon was used at both sides of workpiece to avoid the oxidation of liquid metal. The laser beam irradiated the workpiece vertically, and there was focal spot position at the top surface of the workpiece during laser joining. The angle of  $30^\circ$  between the filler wire and the workpiece was selected. Filler wire was fed in front of the laser beam, as shown in Fig.1. To decrease the difference of heat conductivity and the reflectance of Ti and Al, the offset of laser beam toward Al metal base was set as 0.4 mm.

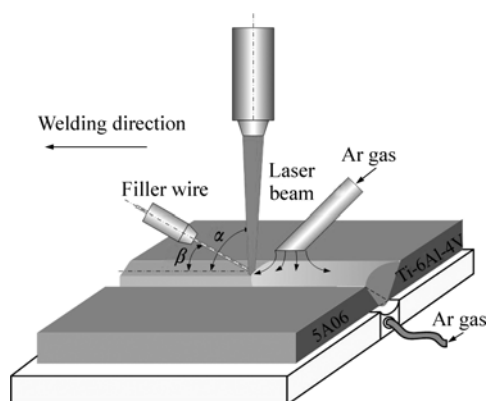


Fig.1 Schematic of laser joining Ti alloy to Al alloy

Ti-6Al-4V and 5A06 Al alloy plates with thickness of 1.5mm were selected as the laser joining materials. The Ti alloy is composed of Al(5.5%–6.8%), V(3.5%–4.5%) (mass fraction) and balance Ti; the 5A06 Al alloy is composed of Mg(5.8%–6.8%), Si(0.4%), Mn(0.5%–0.8%), Fe(0.4%), Zn(0.2%) (mass fraction) and balance Al. And the filler wire with the diameter of 2 mm is composed of Si(12%), Fe(0.8%), Cu(0.3%), Zn(0.2%) (mass fraction) and balance Al.

In this study, standard grinding and polishing sample preparation procedures were used and solutions of 1%HF, 1.5%HCl, 2.5%HNO<sub>3</sub> and 95%H<sub>2</sub>O were used to etch samples. The microstructures of the joint were observed by metallographic microscope and scanning electron microscope (SEM) equipped with an energy-dispersive X-ray spectrometer (EDS) for chemical constitution analysis. The crystal phases of the reaction layer were identified by microbeam X-ray diffractometer, which has advantage of analyzing phase composition in minimum diameter of 50  $\mu\text{m}$ .

### 3 Results and discussion

#### 3.1 Interfacial microstructure in Ti/Al joints

Fig.2 shows typical cross-section morphology of

dissimilar Ti/Al laser welding-brazing joint. It is clear that welding joint has been formed by Al alloy and filler metal, and brazing joint has been formed by Ti alloys and filler metal. According to the observation of interfacial microstructure, there are two joining modes at the interface of Ti/filler metal, i.e., Ti dissolution mode formed by the dissolution of Ti substrate with low heat input and Ti melting mode formed by slight melting of Ti substrate with high heat input.

Under the condition of low heat input, SEM photograph of interfacial microstructure is shown in Fig.3. According to the results of the microbeam XRD,

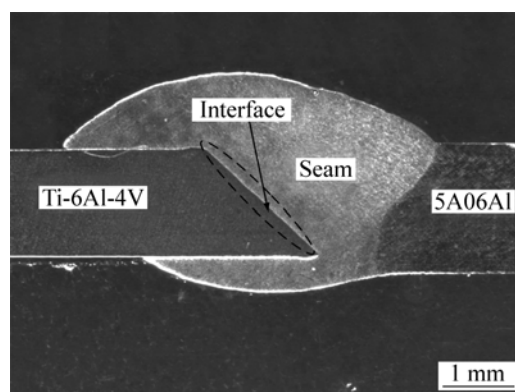


Fig.2 Typical cross-section morphology of dissimilar Ti/Al laser welding-brazing joint

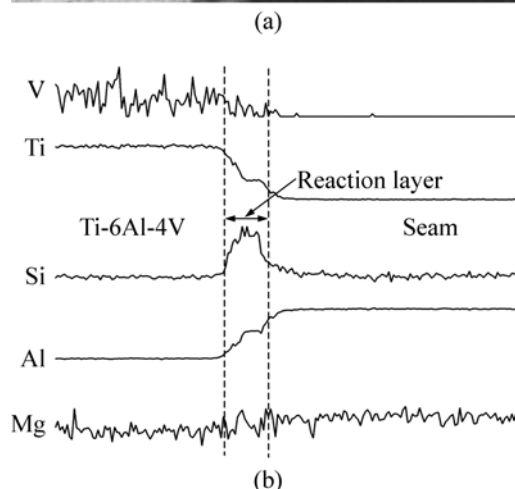
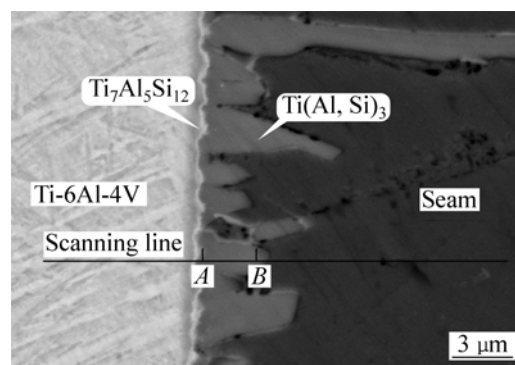
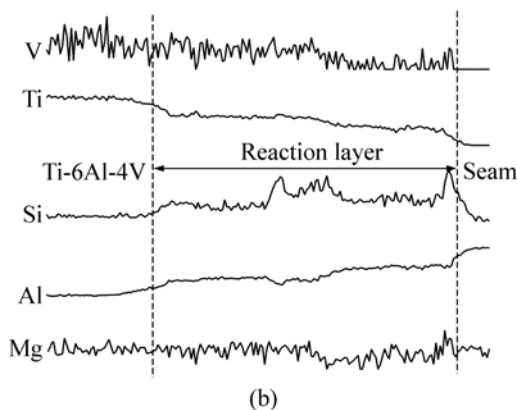
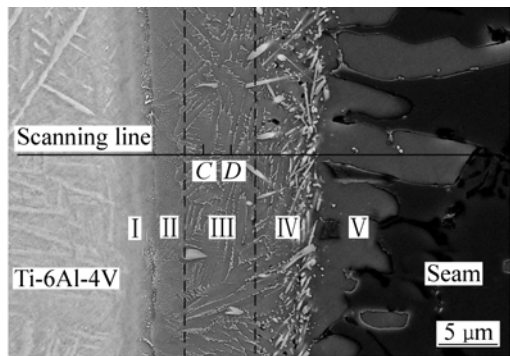


Fig.3 Interfacial microstructure (a) and distribution of elements Ti, Al, Si, Mg and V (b) with dissolution mode

SEM and EDS, there are two reaction layers with discontinuous  $\text{Ti}(\text{Al}, \text{Si})_3$  and continuous  $\text{Ti}_5\text{Si}_3$  at the interface. Intermetallic  $\text{Ti}(\text{Al}, \text{Si})_3$  reaction layer exhibits discontinuous serrate shape. Very thin  $\text{Ti}_5\text{Si}_3$  reaction layer lies between  $\text{Ti}(\text{Al}, \text{Si})_3$  layer and Ti alloy substrate. Fig.3(b) shows the distribution of elements Ti, Al, Si, Mg and V by EDS line scanning at the interface. It is obvious that element Si enriches at the interface between Ti substrate and the filler metal.

With increasing heat input, Ti alloy substrate is melted slightly at the interface. Accordingly, the joining of Al-12Si filler and Ti base metal becomes melting mode. Interfacial microstructure of the joining with melting mode is complex, as shown in Fig.4(a). The thickness of continuous reaction layer increases obviously. According to the results of microbeam XRD and EDS, interfacial microstructure is divided into five layers, i. e. solid-state phase changed reaction layer with  $\text{Ti}_3\text{Al}$  and precipitation  $\text{Ti}_5\text{Si}_3$  ( I ), eutectic reaction layer with  $\text{TiAl}$  and  $\text{Ti}_5\text{Si}_3$  ( II ), hypoeutectic reaction layer with  $\text{Ti}_5\text{Si}_3$  and primary  $\text{TiAl}$  ( III ), hypereutectic reaction layer with primary  $\text{Ti}_5\text{Si}_3$  and  $\text{TiAl}$  ( IV ) and discontinuous reaction layer with  $\text{Ti}(\text{Al}, \text{Si})_3$  ( V ). Granular  $\text{Ti}_5\text{Si}_3$  compounds are surrounded by intermetallic phase  $\text{TiAl}$  in hypereutectic reaction layer. In addition, little  $\text{Ti}_5\text{Si}_3$  particles are precipitated in solid-state phase changed reaction layer close to fusion



**Fig.4** Interfacial microstructure (a) and distribution of elements Ti, Al, Si, Mg and V (b) with melting mode

line, as shown in Fig.5. Fig.4(b) shows the distribution of elements Ti, Al, Si, Mg and V by EDS line scanning at the interface. Similarly, element Si enriches at the interface between Ti substrate and the filler metal.

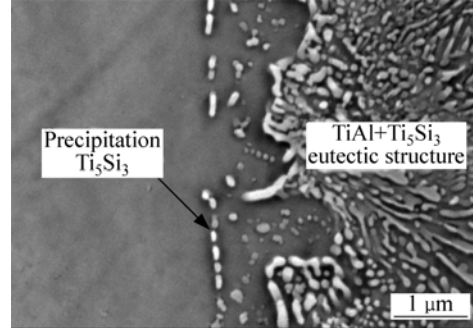


**Fig.5** Morphology of  $\text{Ti}_5\text{Si}_3$  precipitation particles of solid-state phase changed reaction layer in melting mode

The analysis of interfacial microstructure of Ti/Al dissimilar joints shows that Si element participates in formation of the compound  $\text{Ti}_7\text{Al}_5\text{Si}_{12}$  and becomes solutes replacing Al atoms in  $\text{TiAl}_3$  for dissolution mode. For Ti melting mode, Si participates in eutectic, hypoeutectic and hypereutectic reaction and the precipitation of  $\text{Ti}_5\text{Si}_3$  in solid reaction layer. In nature, interfacial reaction mechanism and product formation are affected by the Si diffusion behavior. The Si diffusion behavior will be analyzed from the view of Si chemical potential to explain interfacial mechanism.

### 3.2 Chemical potential prediction model of ternary alloys

During diffusing of the elements, gradient of the chemical potential is a driving force. Element will diffuse to the place where chemical potential is low. Generally, it is difficult to directly calculate or measure the chemical potential. So far, no accurate calculation or measurement of the chemical potential has been reported. Therefore, a model for the prediction of the chemical potential for ternary alloy system is established to analyze the influence of the element content and temperature on Si chemical potential.

As it is known, partial molar free energy, i.e., chemical potential is expressed by

$$\mu_i = \frac{\partial G}{\partial x_i} \quad (1)$$

In fact, free energy  $G$  of real solution is equal to the summation of ideal solution free molar energy  $G^I$  and excess molar free energy  $G^E$ , namely,

$$G = G^I + G^E \quad (2)$$

The mixed free energy of ideal solution is expressed by

$$G^I = G^0 + \Delta G^I = x_i G_i^* + x_j G_j^* + x_k G_k^* + RT(x_i \ln x_i + x_j \ln x_j + x_k \ln x_k) \quad (3)$$

where  $G_i^*$ ,  $G_j^*$  and  $G_k^*$  are molar free energies of pure

component  $i, j, k$ , respectively; and  $x$  is the molar fraction of the component.

The calculation of the excess molar free energy  $G^E$  is a key issue in the established model. It is impossible that  $G^E$  of ternary system is calculated accurately by traditional thermodynamic theory. Thus, Toop equation is used to evaluate the excess free energy of ternary alloys by using that of binary alloys. In ternary system  $i-j-k$ , where  $j$  and  $k$  are symmetry components and  $i$  is asymmetry component, according to excess molar free energies of binary alloys  $G_{ij}^E$ ,  $G_{jk}^E$  and  $G_{ik}^E$ , the excess molar free energy  $G^E$  of ternary system alloys is obtained from Toop equation[11–12]:

$$G^E = \frac{x_j}{1-x_i} G_{ij}^E(x_i, 1-x_i) + \frac{1-x_i-x_j}{1-x_i} G_{ik}^E(x_i, 1-x_i) + (1-x_i)^2 G_{jk}^E\left(\frac{x_j}{1-x_i}, \frac{1-x_i-x_j}{1-x_i}\right) \quad (4)$$

In this way, questions are used to calculate the excess molar free energy  $G^E$  of ternary system to translate the excess molar free energy  $G_{ij}^E$ ,  $G_{jk}^E$  and  $G_{ik}^E$  of binary system. Under the condition of changeless temperature, free energy of binary system is

$$G_{ij}^E = \Delta H_{ij} - T \Delta S_m^E \quad (5)$$

where  $\Delta H_{ij}$  and  $\Delta S_m^E$  are solution enthalpy and excess entropy of binary system, respectively.

Based on the relationship of excess entropy with solution enthalpy established by TANAKA et al[13], there is

$$S_m^E = \Delta H_{ij}(1/T_{m,i} + 1/T_{m,j})/14 \quad (6)$$

where  $T_{m,i}$  and  $T_{m,j}$  are melting points of components  $i$  and  $j$ , respectively.

Therefore, excess molar free energy of binary alloys becomes

$$G_{ij}^E = \Delta H_{ij}[1 - T(1/T_{m,i} + 1/T_{m,j})/14] \quad (7)$$

According to Eq.(7), the excess free energy  $G_{ij}^E$  of binary system is calculated by solution enthalpy  $\Delta H_{ij}$ . Further, the excess free energy  $G^E$  of ternary system is obtained by Eq.(4). Besides elements O, S, Se and Te, for any two elements  $i$  and  $j$ , the solution enthalpy expression is shown by MIEDEMA model of solution enthalpy[14]:

$$\Delta H_{i,j} = f_{ij} \cdot \frac{x_i[1 + \mu_i x_j(\phi_i - \phi_j)]x_j[1 + \mu_j x_i(\phi_j - \phi_i)]}{x_i V_i^{2/3}[1 + \mu_i x_j(\phi_i - \phi_j)] + x_j V_j^{2/3}[1 + \mu_j x_i(\phi_j - \phi_i)]} \quad (8a)$$

$$f_{ij} = \frac{2pV_i^{2/3}V_j^{2/3}[q/p(\Delta n_{WS}^{1/3})^2 - (\Delta\phi)^2 - a(r/p)]}{(n_{WS}^{1/3})_i^{-1} + (n_{WS}^{1/3})_j^{-1}} \quad (8b)$$

where  $x$  is the molar fraction of element;  $\phi$  is the electronegativity;  $V$  is the molar volume;  $n_{WS}$  is the electron density; and  $q, r, \mu, a, p$  are experimental constants, whose physical significances and values are described in detail elsewhere[14].

Therefore, according to Eqs.(1)–(8), chemical potential prediction model of ternary alloys is established. The mixed free energy of Ti-Al-Si ideal solution is obtained by Eq.(3) and the excess free energy  $G^E$  of this system is obtained according to Eqs.(4)–(8). Finally, Si chemical potential of this system is calculated by Eqs.(1) and (2).

### 3.3 Analysis of Si diffusion behavior at interface during laser joining

#### 3.3.1 Calculation of Si chemical potential in Ti-Al-Si system

In this study, the melting points of Ti and Al are around 1 900 and 900 K, respectively. According to prediction model of ternary alloy, Si chemical potential dependent on molar fraction of Ti and Si is calculated for dissolution mode (1 000 K) and melting mode (2 000 K), as shown in Fig.6. Therefore, Si diffusion behavior is analyzed according to relationship of Si chemical potential with some factors, for example, element content and temperature.

#### 3.3.2 Si diffusion behavior for Ti dissolution mode

In this study, there is 12% Si (mass fraction) in filler

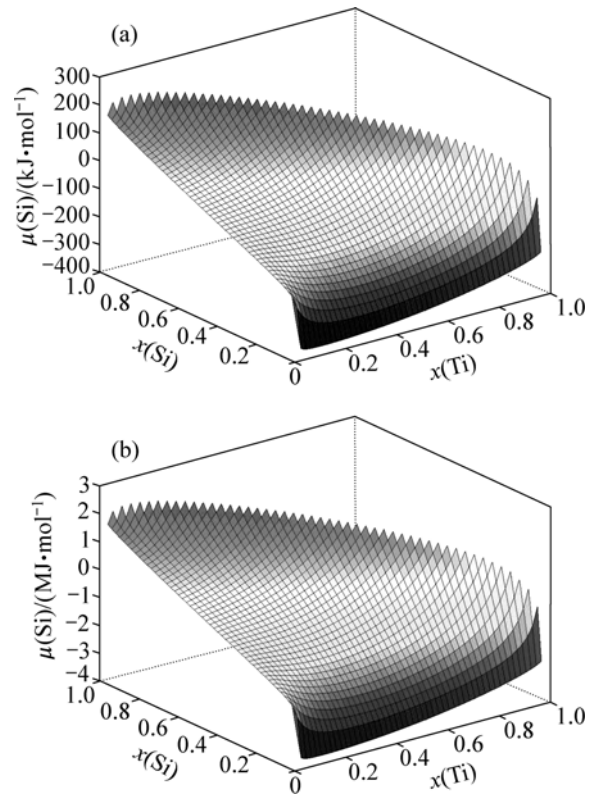


**Fig.6** Si chemical potential dependent on molar fraction of Ti and Si in dissolution mode (1 000 K) (a) and melting mode (2 000 K) (b)

Ai-12Si (molar fraction of 0.116). This means that ratio of Al to Si in liquid filler is always remained during Ti dissolution. Thus, the influence of Ti molar fraction on Si chemical potential was analyzed during laser joining under this ratio.

The relationship curves of Si chemical potential  $\mu(\text{Si})$  with Ti molar fraction  $x(\text{Ti})$  was calculated, as shown in Fig.7. It is clear that critical point of Ti molar fraction is 0.5 at almost all temperatures. With increasing Ti molar fraction, Si chemical potential decreases when this fraction is lower than 0.5 and increases when it is higher than 0.5. As shown in Fig.7, Si chemical potential tends to decrease with increasing temperature. However, the influence of Ti molar fraction is far higher than that of the temperature on Si chemical potential. Therefore, the attention is focused on the influence of the Ti content distribution on Si chemical potential.

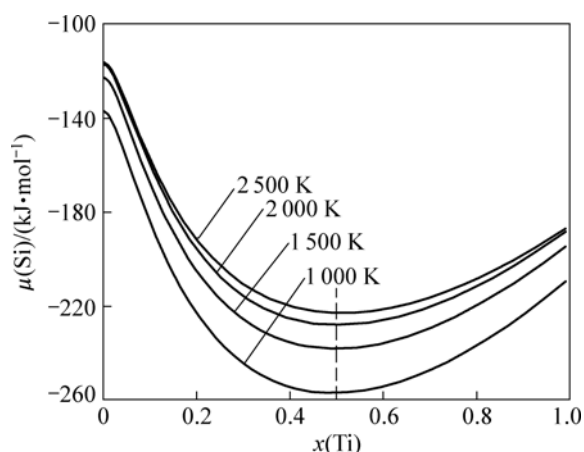


**Fig.7** Relationship curves of Si chemical potential with Ti molar fraction

In Ti dissolution mode, element distribution between *A* and *B* points in Fig.3(a) is shown in Table 1. It is obvious that Ti molar fraction is lower than 0.5 in Table 1. This means that Si chemical potential decreases with increasing Ti molar fraction during joining for Ti dissolution mode. In liquid filler near the interface, Ti content is the highest, which leads to the reduction of Si chemical potential. Therefore, Si atom in liquid filler diffuses to the interface during laser joining, and then Si gathering phenomena appear at the interface.

During interfacial reaction, Si gathering phenomena and Ti dissolution induce the formation of Si-rich compound  $\text{Ti}_7\text{Al}_5\text{Si}_{12}$  at the interface. The formation of this compound wastes a number of Si atoms, which induces the reduction of Si content at the interface. Therefore, intermetallic  $\text{TiAl}_3$  is formed in the form of crystallization. Considering the gathering phenomena of Si atoms, up to 15% Al can be replaced by silicon in  $\text{TiAl}_3$  lattice structures due to the adjacent atomic radii, and it can be commonly written as  $\text{Ti}(\text{Al}, \text{Si})_3$ [15].

**Table 1** Element content distribution in reaction layer for Ti dissolution mode

Distance/ $\mu\text{m}$	$x(\text{Mg})/\%$	$x(\text{Al})/\%$	$x(\text{Si})/\%$	$x(\text{Ti})/\%$	$x(\text{V})/\%$
8.02	1.12	59.07	9.38	28.7	1.73
8.2	1.28	58.6	8.81	30.98	0.33
8.39	0.45	61.35	8.83	28.96	0.41
8.58	0.78	60.28	11.66	25.17	2.11
8.76	1.36	60.22	11.15	26.5	0.78
8.95	0.54	60.08	10.99	28.39	0
9.13	0.89	62.14	11.79	25.18	0
9.32	1.44	66.23	9.79	21.67	0.87
9.51	1.11	67.03	8.65	23.21	0
9.69	0.91	67.75	6.67	23.86	0.8

### 3.3.3 Si diffusion behavior for Ti dissolution mode

In the case of melting mode, Ti substrate is melted slightly at the interface due to high heat input, which means contact of liquid Ti with liquid filler. Thus, smart diffusion process appears also in liquid Ti besides liquid filler. Two zones with liquid filler and liquid Ti at the interface are divided to analyze Si diffusion behavior, as shown in Fig.8.

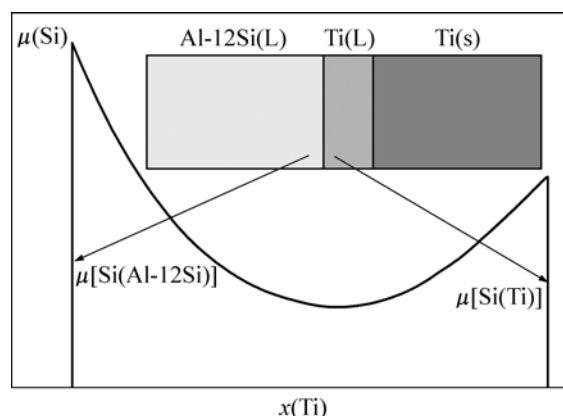


**Fig.8** Schematic diagram of diffusion process for melting mode

In liquid filler zone, the Si diffusion behavior is similar with dissolution mode. Si chemical potential decreases in liquid filler due to the diffusion of the liquid Ti to the filler. Thus, Si atom will enrich at the interface from liquid filler.

In the liquid Ti zone, the Si chemical potential,  $\mu[\text{Si}(\text{Al-12Si})]$ , in liquid filler ( $x(\text{Ti})=0$ ) is far higher than  $\mu[\text{Si}(\text{Ti})]$  in liquid Ti ( $x(\text{Ti})=1$ ), as shown in Fig.8. This indicates that the Si and Al atoms diffuse strongly to liquid Ti from filler due to the drive of the chemical potential gradient. Clearly, the ratio of Al or Si in liquid Ti is different with liquid filler at early stage of the diffusion. Thus, Si chemical potential is influenced by Si and Ti contents. Fig.9 shows the relationship of Si chemical potential with Si content under the condition of the same Ti molar fraction. As shown in Fig.9, Si chemical potential decreases with the reduction of Si

molar fraction in the case of the same Ti content for Ti-Al-Si ternary system. Under the condition of the same Si content, Si chemical potential decreases with increasing Ti molar fraction. It is shown that Si atom tends to diffuse to the zone with low Si and high Ti molar fraction for Ti-Al-Si ternary system. During welding, Si content decreases and Ti content increases with increasing distance from the interface in liquid Ti. Therefore, Si atom diffuses to inner zone of liquid Ti during laser joining for melting mode.

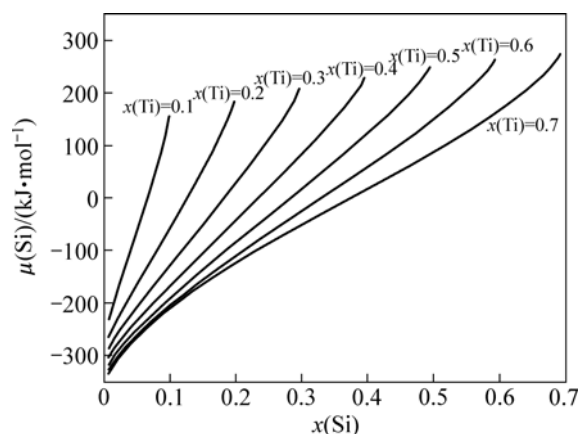


**Fig.9** Influence of Si molar fraction on Si chemical potential for same Ti content

In addition, Si and Ti contents in liquid Ti increase continuously with progress of the diffusion. Finally, the ratio of Al or Si in liquid Ti is the same with that in liquid filler because the bulk of liquid filler is far larger than that of liquid Ti. Therefore, Si chemical potential can reach the minimum value, as shown in Fig.7, when Ti molar fraction is around 0.5. Element distribution between *C* and *D* points in Fig.4(a) is shown in Table 2. It is obvious that Ti molar fraction is around 0.5 and ratio of Al or Si is close to that in liquid filler, which indicates that prediction model of chemical potential is proper.

There is complex metallurgical reaction at the interface during the diffusion. According to above five

**Table 2** Element distribution in reaction layer for Ti melting mode

Distance/ $\mu\text{m}$	$x(\text{Mg})/\%$	$x(\text{Al})/\%$	$x(\text{Si})/\%$	$x(\text{Ti})/\%$	$x(\text{V})/\%$
15.15	1.3	41.79	3.35	51.03	2.52
15.35	1.75	38.19	3.94	52.21	3.91
15.55	1.01	41.68	3.02	50.14	4.15
15.75	0.93	42.84	3.44	51.17	1.61
15.95	1.69	39.32	6.41	50.73	1.86
16.15	0.76	40.24	4.21	49.51	5.27
16.35	1.44	39.46	4.37	50.38	4.35
16.55	2.11	40.49	3.21	51.66	2.52
16.75	2.11	39.51	4.42	49.25	4.71
16.95	1.54	39.92	4.24	49.7	4.61

layers in melting mode, corresponding interfacial reaction is analyzed as follows.

In zone I, the solid-state phase changes occur in solid Ti alloy substrate near fusion line due to Si and Al diffusion. The solid-state phase changed reaction layer with  $\text{Ti}_3\text{Al}$  and precipitation  $\text{Ti}_5\text{Si}_3$  is formed.

In zone II, eutectic reaction appears in melting Ti alloy near fusion line:  $L \rightarrow \text{TiAl} + \text{Ti}_5\text{Si}_3$ . The filamentous eutectic reaction layer with  $\text{Ti}_5\text{Si}_3$  and TiAl is formed.

In zone IV,  $\text{Ti}_5\text{Si}_3$  as primary phase is formed due to high melting point of  $\text{Ti}_5\text{Si}_3$  and strong combining capability of Si with Ti[16]. Hypereutectic reaction layer with TiAl and primary  $\text{Ti}_5\text{Si}_3$  appears in this zone.

In zone III, because a mass of Si atoms are expended by formation of  $\text{Ti}_5\text{Si}_3$  in hypereutectic reaction layer (zone IV), surrounding Si should diffuse to around reaction zone of  $\text{Ti}_5\text{Si}_3$  formation, which induces appearance of poor Si zone between zone II and IV. Therefore, hypoeutectic structure of  $\text{Ti}_5\text{Si}_3$  and primary TiAl is formed in this zone.

In the zone V, with the decrease of temperature, serration-shape reaction layer consisting of  $\text{Ti}(\text{Al}, \text{Si})_3$  forms in crystallization. The formation mechanism of  $\text{Ti}(\text{Al}, \text{Si})_3$  layer is the same as dissolution mode.

## 4 Conclusions

1) In laser joining of Al alloy to Ti alloy, Si element diffuses to the interface and enriches there with the mode of Ti dissolution or melting. It is found that Si diffusion behavior plays an important role in forming those interfacial compounds.

2) Chemical potential prediction model of the ternary alloys is established based on MIEDEMA model of solution enthalpy. The influence of Ti molar fraction and temperature on Si chemical potential is analyzed according to calculated results. It is found that the influence of Ti molar fraction is far higher than that of the temperature on Si chemical potential. The minimum value of Si chemical potential is approximate 0.5 of Ti molar fraction, which presents a good agreement with experimental data.

3) In the case of Ti dissolution mode, the dissolution of Ti alloy in liquid filler induces the reduction of the Si chemical potential. This causes the phenomenon of Si element gathering at the interface. In the case of Ti melting mode, element Si not only gets together at the interface, but also further diffuses to liquid Ti due to slight melting of Ti substrate.

## References

- [1] RENDIGS K H. The use of titanium in family automobiles: Current trends [J]. Mater Sci Forum, 1997, 242: 11–24.
- [2] MILLER W S, ZHUANG L, BOTTEMA J, WITTEBROOD A J, de

- SMET P, HASZLER A, VIERGE A. Recent development in aluminium alloys for the automotive industry [J]. *Mater Sci Eng A*, 2000, 280(1): 37–49.
- [3] WEI R J, JIANG L Y, TAO F. Microstructure characteristics in the interface zone of Ti/Al diffusion bonding [J]. *Mater Lett*, 2002, 56(5): 647–652.
- [4] SOHN W H, BONG H H, SOON H. Microstructure and bonding mechanism of Al/Ti bonded joint using Al-10Si-1Mg filler metal [J]. *Mater Sci Eng A*, 2003, 355(1/2): 231–240.
- [5] TAKEMOTO T, OKAMOTO I. Intermetallic compounds formed during brazing of titanium with aluminium filler metals [J]. *J Mater Sci*, 1988, 23(4): 1301–1308.
- [6] ZHU Y, ZHAO P F, KANG H, HU G, QU P. A preliminary study on filler metals for vacuum brazing of Al/Ti [J]. *China Welding*, 2002, 11(2): 130–132.
- [7] KIM Y C, FUJI A. Joint characteristics in Ti-Al friction welds [J]. *Science and Technology of Welding and Joining*, 2002, 7: 149–154.
- [8] KAHRAMAN N, GULENC B, FINDIK F. Corrosion and mechanical microstructural aspects of dissimilar joints of Ti-6Al-4V and Al plates [J]. *International Journal of Impact Engineering*, 2007, 34: 1423–1432.
- [9] CHEN Shu-hai, LI Li-qun, CHEN Yan-bin. Welding characteristics of Al/Ti dissimilar alloys using laser welding-brazing with different spot [J]. *Transactions of the China Welding Institution*, 2008, 29(6): 49–52. (in Chinese)
- [10] CHEN Shu-hai, LI Li-qun, CHEN Yan-bin. Interface characteristic and property of Ti/Al dissimilar alloys joint with laser welding-brazing [J]. *The Chinese Journal of Nonferrous Metal*, 2008, 18(6): 991–996. (in Chinese)
- [11] TOOP G W. Predicting ternary activities using binary data [J]. *Trans Metall Soc AIME*, 1965, 233(5): 850–854.
- [12] PELTON A D, THOMPSON W T. Phase diagrams [J]. *Prog Solid State Chem*, 1975, 10(3): 119–123.
- [13] TANAKA T, GOKCEN N A, MORITA Z. Relationship between enthalpy of mixing and excess entropy in liquid binary alloys [J]. *Z Metallkde*, 1990, 81(1): 49–58.
- [14] MIEDEMA A R, de CHATEL P F, de BOER F R. Cohesion in alloys-fundamentals of a semi-empirical model [J]. *Physica*, 1980, 100B: 1–28.
- [15] GUPTA S P. Intermetallic compounds in diffusion couples of Ti with an Al-Si eutectic alloy [J]. *Mater Charact*, 2003, 49: 321–330.
- [16] XIONG H P, XIE Y H, MAO W, MA W L, CHEN Y F, LI X H, CHENG Y Y. Improvement in the oxidation resistance of the TiAl-based alloy by liquid-phase siliconizing [J]. *Scripta Materialia*, 2003, 49: 1117–1122.

(Edited by YANG Bing)